The Effect of Discrete Δx on Wave Migration Accuracy

by Walter S. Lynn

The migration of seismic data using the wave equation requires the use of approximations to the wave equation. Which approximation to use is usually a compromise between accuracy and cost. There are two errors involved with wave equation migration. One is caused by anisotropic dispersion, which means waves traveling in different directions propagate at different velocities. This is an artifact of our approximations to the wave equation. The other error is due to frequency dispersion which is caused by undersampling the data. In this paper we will examine the effect of sampling the x dimension on the accuracy of the 15° and 45° approximations.

The results are displayed in several ways. We will first examine the effect on the dispersion relation of the exact one way wave equation. Next we will see what happens to the dispersion relations, group velocities and travel time curves of the 15° and 45° equations. Finally, we will examine the x and time errors ("knots") in migrating an ideal hyperbola. There is a considerable amount of overlap in the information displayed in each type of plot. As a result something which might be seen as confusing in one figure can often be explained by referring to its counterpart in another figure.

The effect of discrete Δx on the exact one-way wave equation.

Fourier transforming the exact wave equation gives the dispersion relation for upcoming waves

$$\frac{v\,k_z}{\omega} = -\left(1 - \frac{v^2 k^2}{\omega^2}\right)^{1/2} , \qquad (1)$$

where $k = k_x$.

Equation (1) describes the well known semi-circle in k_x , k_z space. To obtain the necessary approximations to the wave equation we replace the square root in (1) by various rational fraction approximations. When the x coordinate is discretized, the ∂_{xx} term in the wave equation becomes $\delta_{xx} / \Delta x^2$, where $\delta_{xx} = (1, -2, 1)$. If we If we denote the effective wave number in the x direction as $\hat{k}$, then Fourier transforming both operators gives

$$\hat{k} = \frac{2}{\Delta x} \sin\left(\frac{k\,\Delta x}{2}\right) \qquad (2)$$

An alternative relation between k and $\hat{k}$ which is given by approximating $i\,k$ with the bilinear transform is

$$\hat{k} = \frac{2}{\Delta x} \tan\left(\frac{k\,\Delta x}{2}\right) \qquad (3)$$

The derivation of these equations is given in Claerbout's book on pages 221-222. The effective horizontal wave number is now periodic with k . Whether equation (2) or (3) is to be used depends upon the finite differencing scheme. It is also possible for $\hat{k}$ to be some combination of (2) and (3).

Substituting (2) and (3) into (1) gives the effective vertical wave number in terms of k

$$\frac{v\,\hat{k}_z}{\omega} = -\left[\,1 - \left(\frac{2v}{\omega\Delta x} \sin\left(\frac{\omega\Delta x}{2v}\;\frac{vk}{\omega}\right)\right)^2\,\right]^{1/2} \qquad (4a)$$

and

$$\frac{v\,\hat{k}_z}{\omega} = -\left[\,1 - \left(\frac{2v}{\omega\Delta x} \tan\left(\frac{\omega\Delta x}{2v}\;\frac{vk}{\omega}\right)\right)^2\,\right]^{1/2} \qquad (4b)$$

The dispersion relation is now periodic with a period of $m = \frac{2v}{\omega \Delta x} \pi$. Figure 1 shows the graphs of these curves over a range of m's . Note the different direction of departures from the ideal semi-circle of the sine and tangent relations for decreasing m . In the former case, the limbs of the semi-circle are stretched out and begin to overlap at $m = \pi$. In the latter case, the limbs are compressed towards the k_z axis.

To see where we stand a typical value for m is

$$m = \frac{2\,(3000\ \text{m/sec})\,\pi}{2\pi(60\ \text{hz})(50\ \text{m})} = 1$$

This is well below the lowest value of m in Figure 1 and indicates a gross undersampling in the x direction. This creates a severe aliasing problem in the spatial frequency domain. We will see shortly that the problem becomes much more severe when we approximate the wave equation.

Effect of discrete Δx on approximations to the wave equation.

Various orders of approximations to the one-way wave equation are obtained by different orders of rational approximations to the square root in (1). We will now generalize to the slant frame coordinate system defined by

$$x' = x + z \tan\theta$$

$$z' = z$$

and

$$t' = t + \frac{z}{v}\cos\theta - \frac{x}{v}\sin\theta$$

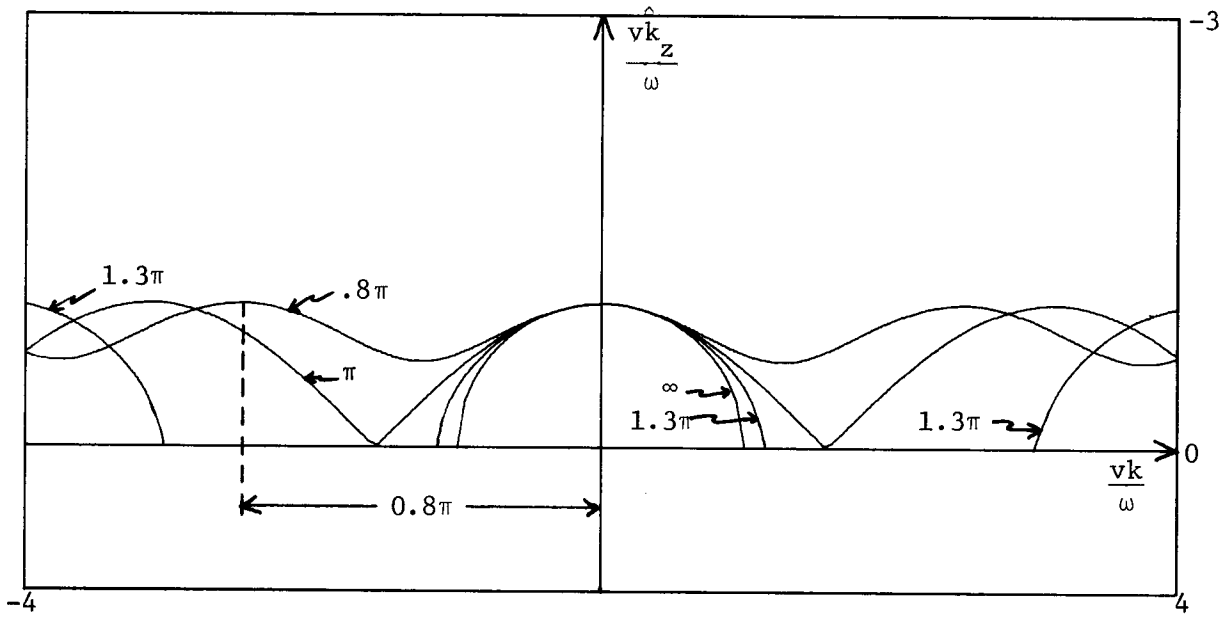

a

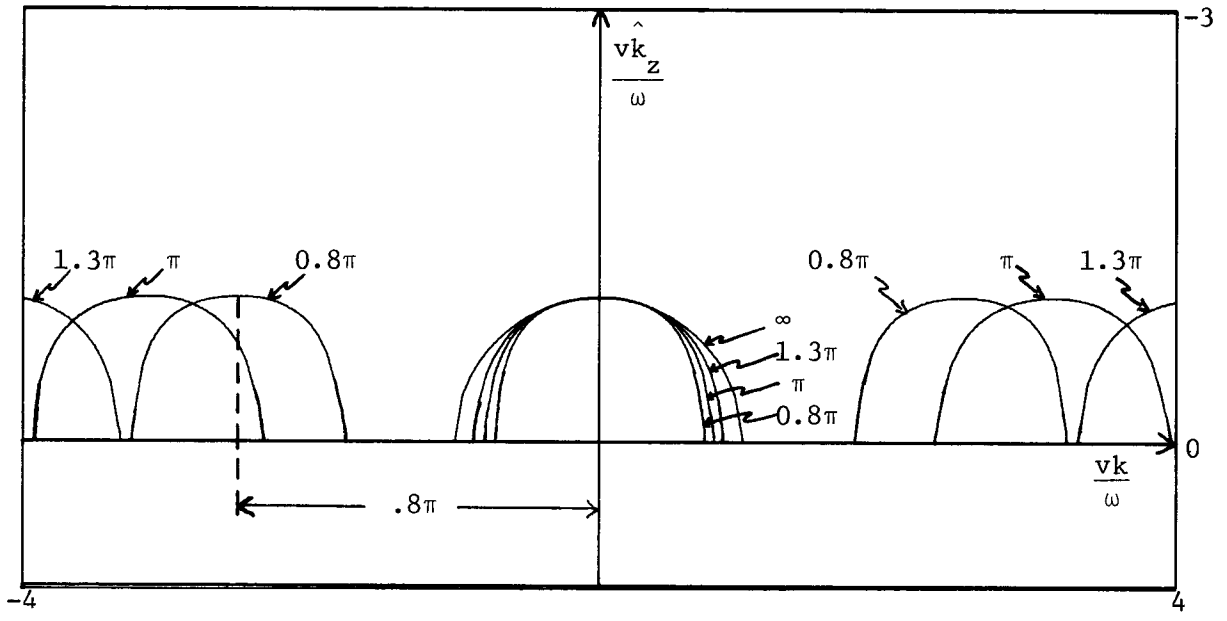

b

Figure 1. The effect of sampling x on the dispersion relation for the exact one-way wave equation. m is a dimensionless number equal to $\frac{2v}{\omega \Delta x} \pi$ which is the period of the dispersion relation. Equation plotted is $\frac{\hat{vk}_z}{\omega} = -(1 - \frac{v^2\hat{k}^2}{\omega^2})^{1/2}$ for a) $\hat{k} = \frac{2}{\Delta x} \sin(\frac{k \Delta x}{2})$ and b) $\hat{k} = \frac{2}{\Delta x} \tan(\frac{k \Delta x}{2})$.

Derived below are the necessary adjustments to Claerbout's program (SEP-8, page 29) to account for the discretization of the x axis. We start with the following definition and relations:

$$Y = \frac{v\,k'}{\omega'\cos\theta} = \left(\frac{vk}{\omega} - \sin\theta\right) / \cos\theta$$

$$k'_z = \frac{T(Y)}{B(Y)}\,\frac{\omega'\cos\theta}{v}$$

and

$$k'_z = \frac{T(Y)}{B(Y)}\,\frac{\omega\cos\theta}{v} + k\tan\theta - \frac{\omega}{v\cos\theta}$$

These equations are derived by Claerbout on page 21 . For discrete x , define

$$\hat{Y} = \frac{v\,\hat{k}'}{\omega'\cos\theta} = \frac{2v}{\omega'\,\Delta x\cos\theta}\sin\left(\frac{vk'}{\omega}\,\frac{\omega'\,\Delta x}{2v}\right)$$

$$= \frac{2v}{\omega\,\Delta x\cos\theta}\sin\left[\left(\frac{vk}{\omega} - \sin\theta\right)\frac{\omega\,\Delta x}{2v}\right]$$

The effective vertical wave numbers are given by:

$$\hat{k}'_z = \frac{T(\hat{Y})}{B(\hat{Y})}\,\frac{\omega'\cos\theta}{v} \qquad (5a)$$

and

$$\hat{k}_z = \frac{T(\hat{Y})}{B(\hat{Y})}\,\frac{\omega\cos\theta}{v} + k\tan\theta - \frac{\omega}{v\cos\theta} \qquad (5b)$$

In order to display the group velocity and travel time curves we need the following partial derivatives:

$$\frac{\partial\hat{k}'_z}{\partial k'}\,,\quad \frac{\partial\hat{k}'_z}{\partial\omega'}\,,\quad \frac{\partial\hat{k}_z}{\partial k}\,,\quad \frac{\partial\hat{k}_z}{\partial\omega}$$

A preliminary step is to evaluate the partial derivatives of Y with respect to k', ω', k and ω. These are

$$\frac{\partial \hat{Y}}{\partial k'} = \frac{v}{\omega' \cos\theta} \cos\left(\frac{vk'}{\omega'} \frac{\omega' \Delta x}{2v}\right) , \tag{6a}$$

$$\frac{\partial \hat{Y}}{\partial \omega'} = \frac{-\hat{Y}}{\omega'} , \tag{6b}$$

$$\frac{\partial \hat{Y}}{\partial k} = \frac{v}{\omega \cos\theta} \cos\left[\left(\frac{vk}{\omega} - \sin\theta\right)\frac{\omega \Delta x}{2v}\right] , \tag{6c}$$

$$\frac{\partial \hat{Y}}{\partial \omega} = \frac{-\hat{Y}}{\omega} - \frac{\tan\theta}{\omega} \cos\left[\left(\frac{vk}{\omega} - \sin\theta\right)\frac{\omega \Delta x}{2v}\right] . \tag{6d}$$

The necessary partial derivatives are obtained by differentiating (5a,b) with respect to the desired variable and using equations (6a,b,c,d). Thus,

$$\hat{s}'_{k'} = \frac{\partial \hat{k}'_z}{\partial k'} = \frac{\partial}{\partial \hat{Y}}\left(\frac{T}{B}\right) \frac{\partial \hat{Y}}{\partial k'} \frac{\omega' \cos\theta}{v}$$

$$\hat{s}'_{k'} = \frac{\partial}{\partial \hat{Y}}\left(\frac{T}{B}\right) \cos\left(\frac{vk'}{\omega'} \frac{\omega' \Delta x}{2v}\right) , \tag{7a}$$

$$\hat{s}'_{\omega'} = \frac{\partial \hat{k}'_z}{\partial \omega'} = \left[\frac{T}{B} + \omega' \frac{\partial}{\partial \hat{Y}}\left(\frac{T}{B}\right) \frac{\partial Y}{\partial \omega'}\right] \frac{\cos\theta}{v}$$

$$\hat{s}'_{\omega'} = \left[\frac{T}{B} - \hat{Y} \frac{\partial}{\partial \hat{Y}}\left(\frac{T}{B}\right)\right] \frac{\cos\theta}{v} , \tag{7b}$$

$$\hat{s}_k = \frac{\partial \hat{k}_z}{\partial k} = \frac{\partial}{\partial \hat{Y}}\left(\frac{T}{B}\right) \frac{\partial \hat{Y}}{\partial k} \frac{\omega \cos\theta}{v} + \tan\theta$$

$$\hat{s}_k = \frac{\partial}{\partial \hat{Y}}\left(\frac{T}{B}\right) \cos\left[\left(\frac{vk}{\omega} - \sin\theta\right)\frac{\omega \Delta x}{2v}\right] + \tan\theta , \tag{7c}$$

and

$$\hat{s}_{\omega} = \frac{\partial \hat{k}_z}{\partial \omega} = \left[\frac{T}{B} + \omega \frac{\partial}{\partial \hat{Y}} \left(\frac{T}{B}\right) \frac{\partial \hat{Y}}{\partial \omega} \right] \frac{\cos\theta}{v} - \frac{1}{v \cos\theta}$$

$$\hat{s}_{\omega} = \left[\frac{T}{B} - \frac{\partial}{\partial \hat{Y}} \left(\frac{T}{B}\right) \left\{ \hat{Y} + \tan\theta \cos\left[\left(\frac{kv}{\omega} - \sin\theta \right) \frac{\omega \Delta x}{2v} \right] \right\} \right] \frac{\cos\theta}{v}$$

$$- \frac{1}{v \cos\theta} \quad . \tag{7d}$$

A similar sequence of steps leads to the following expressions if we use $\hat{k}_x = \frac{2}{\Delta x} \tan\left(\frac{k \Delta x}{2}\right)$,

$$\hat{s}'_{k'} = \frac{\partial}{\partial \hat{Y}} \left(\frac{T}{B}\right) / \cos^2 \left(\frac{vk'}{\omega'} \frac{\omega' \Delta x}{2v}\right) \quad , \tag{8a}$$

$$\hat{s}'_{\omega'} = \left[\frac{T}{B} - \hat{Y} \frac{\partial}{\partial \hat{Y}} \left(\frac{T}{B}\right) \right] \frac{\cos\theta}{v} \quad , \tag{8b}$$

$$\hat{s}_{k} = \frac{\partial}{\partial \hat{Y}} \left(\frac{T}{B}\right) / \cos^2 \left[\left(\frac{vk}{\omega} - \sin\theta \right) \frac{k \Delta x}{2v} \right] + \tan\theta \quad , \tag{8c}$$

and

$$\hat{s}_{\omega} = \left[\frac{T}{B} - \frac{\partial}{\partial \hat{Y}} \left(\frac{T}{B}\right) \left\{ \hat{Y} + \tan\theta / \cos^2 \left[\left(\frac{vk}{\omega} - \sin\theta \right) \frac{k \Delta x}{2v} \right] \right. \right. \frac{\cos\theta}{v}$$

$$- \frac{1}{v \cos\theta} \tag{8d}$$

Figures 2 (a,b) show the necessary changes to subroutine EVAL on page 29 to calculate these derivatives for the sine and tangent approximations.

We are now in a position to examine the effect of discretizing the x axis on the phase velocity, group velocity and the x vs. t travel time curves.

```
      SUBROUTINE EVAL(THETAZ,N,T,B,SINTH,S,SK,SK,SPM,SPK,SP)
      DIMENSION T(20),B(20)
      SINZ=SIN(THETAZ)
      COSZ=COS(THETAZ)
      TANZ=SINZ/COSZ
      Y=SINTH-SINZ
      YHAT=SP*SIN(Y/SP)/COSZ
      COSY=COS(Y/SP)
      TOP=0
      BOT=0
      DO 30 I=1,N
      IR=N-I+1
      TOP=T(IR)+TOP*YHAT
   30 BOT=B(IR)+BOT*YHAT+1.E-20
      S=COSZ*TOP/BOT+TANZ*SINTH-1./COSZ
      TOPD=0
      BOTD=0
      DO 40 I=2,N
      IR=N-I+2
      TOPD=(IR-1)*T(IR)+TOPD*YHAT
   40 BOTD=(IR-1)*B(IR)+BOTD*YHAT
      DRAT=TOPD/BOT-TOP*BOTD/(BOT*BOT)
      SK=COSZ*(TOP/BOT-DRAT*(YHAT+TANZ*COSY))-1./COSZ
      SK=DRAT*COSY+TANZ
      SPM=COSZ*(TOP/BOT-DRAT*YHAT)
      SPK=DRAT*COSY
      RETURN
      END
```

$\frac{2V}{\omega \Delta x}$

definition of $\hat{Y}$

} substitute $\hat{Y}$ for Y

} substitute $\hat{Y}$ for Y

eqn 7d

eqn 7c

eqn 7b

eqn 7a

Figure 2a. Modifications to subroutine EVAL for $\hat{k} = \frac{2}{\Delta x} \sin\left(\frac{k \Delta x}{2}\right)$.

Evaluates $\hat{s}'_k$, , $\hat{s}'_\omega$, , $\hat{s}_k$, and $\hat{s}_\omega$.

```
      SUBROUTINE EVAL(THETAZ,N,T,B,SINTH,S,SM,SK,SPW,SPK,SP)
      DIMENSION T(20),B(20)
      SINZ=SIN(THETAZ)
      COSZ=COS(THETAZ)
      TANZ=SINZ/COSZ
      Y=SINTH-SINZ
      YHAT=SP*TAN(Y/SP)/COSZ
      COSY=COS(Y/SP)
      COSY2=COSY**2
      TOP=0
      BOT=0
      DO 30 I=1,N
      IR=N-I+1
      TOP=T(IR)+TOP*YHAT
30    BOT=B(IR)+BOT*YHAT+1.E-20
      S=COSZ*TOP/BOT+TANZ*SINTH-1./COSZ
      TOPD=0
      BOTD=0
      DO 40 I=2,N
      IR=N-I+2
      TOPD=(IR-1)*T(IR)+TOPD*YHAT
40    BOTD=(IR-1)*B(IR)+BOTD*YHAT
      DRAT=TOPD/BOT-TOP*BOTD/(BOT*BOT)
      SM=COSZ*(TOP/BOT-DRAT*(YHAT+TANZ/COSY2))-1./COSZ
      SK=DRAT/COSY2+TANZ
      SPW=COSZ*(TOP/BOT-DRAT*YHAT)
      SPK=DRAT/COSY2
      RETURN
      END
```

$\frac{2V}{\omega \Delta x}$

definition of $\hat{Y}$

} substitute $\hat{Y}$ for Y

} substitute $\hat{Y}$ for Y

eqn 8d

eqn 8c

eqn 8b

eqn 8a

Figure 2b. Modifications to subroutine EVAL for $\hat{k} = \frac{2}{\Delta x} \tan\left(\frac{k \Delta x}{2}\right)$.

Following equations (35 a,b,c) on page 26 we have

$$(x,t) = (\hat{s}_k, -\hat{s}_\omega) \tag{9a}$$

$$(x',t') = (\hat{s}'_{k'}, -\hat{s}'_{\omega'}) \tag{9b}$$

$$(x, -z) = (-\hat{s}_k/\hat{s}_\omega, -1/\hat{s}_\omega) \quad . \tag{9c}$$

For the time being, we will restrict ourselves to the second and third order (15° and 45°) approximations and the case $\theta = 0$.

Phase velocity.

The dispersion relation for the exact one-way wave equation is a semi-circle as shown in Figure 1 (for $m = \infty$). If the operator $\delta_{xx} = (1, -2, 1)$ is used for ∂_{xx} then the effect on the dispersion relation is as shown in Figure 3. Figure 3a represents the effect of discretizing x on the 15° approximation and Figure 3b, the 45° approximation. The range of $\frac{kv}{\omega}$ is -4 to 4 for this and subsequent figures. Curves for 5 different m's are plotted on each figure with $m = \infty$ representing the best fit to the exact wave equation.

The effect of discretizing x can best be seen by comparing Figures 1a and 3. Consider the curve for $m = 1.3\pi$ and recall that m is the periodicity of the dispersion relation. For the exact wave equation (Fig. 1a), the dispersion relation diverges slightly from the ideal semi-circle and $\frac{vk_z}{\omega}$ becomes imaginary at $\frac{vk}{\omega} = \pm 1.132$. For the 15° equation (Fig. 3a), the aliasing effect becomes more severe and the curve diverges even more from the ideal semi-circle. That $\frac{v\hat{k}_z}{\omega}$ is real for all $\frac{vk}{\omega}$ is a property of the approximations to the wave equation; however, whether $\frac{v\hat{k}_z}{\omega}$ is positive or negative is highly

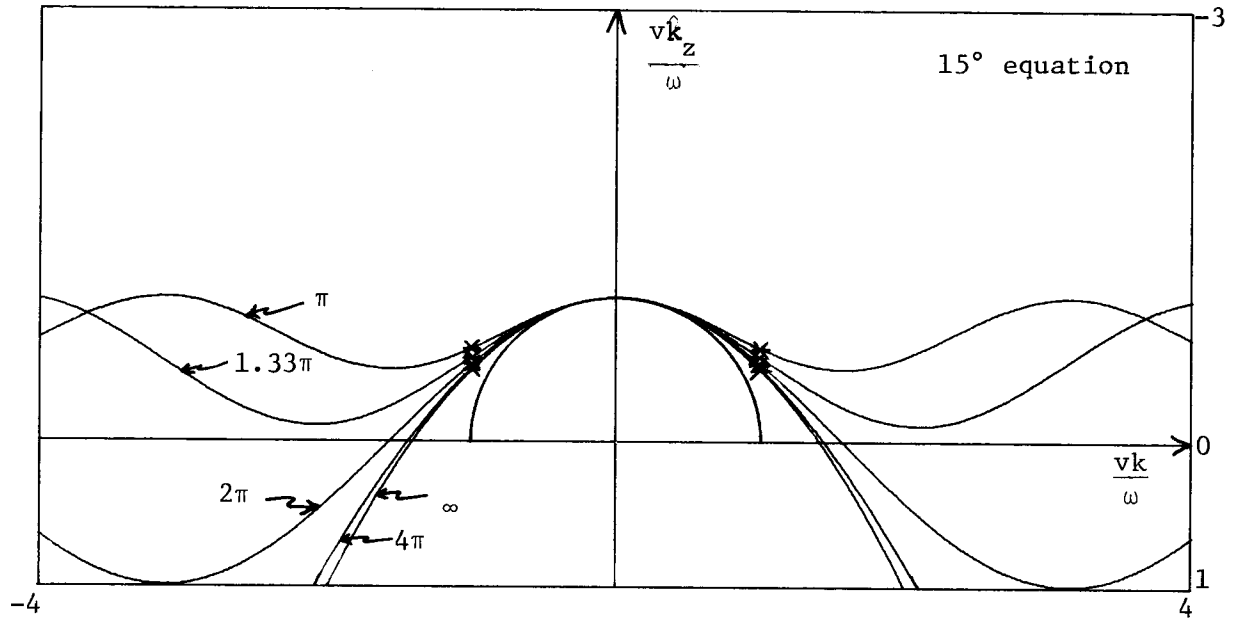

a

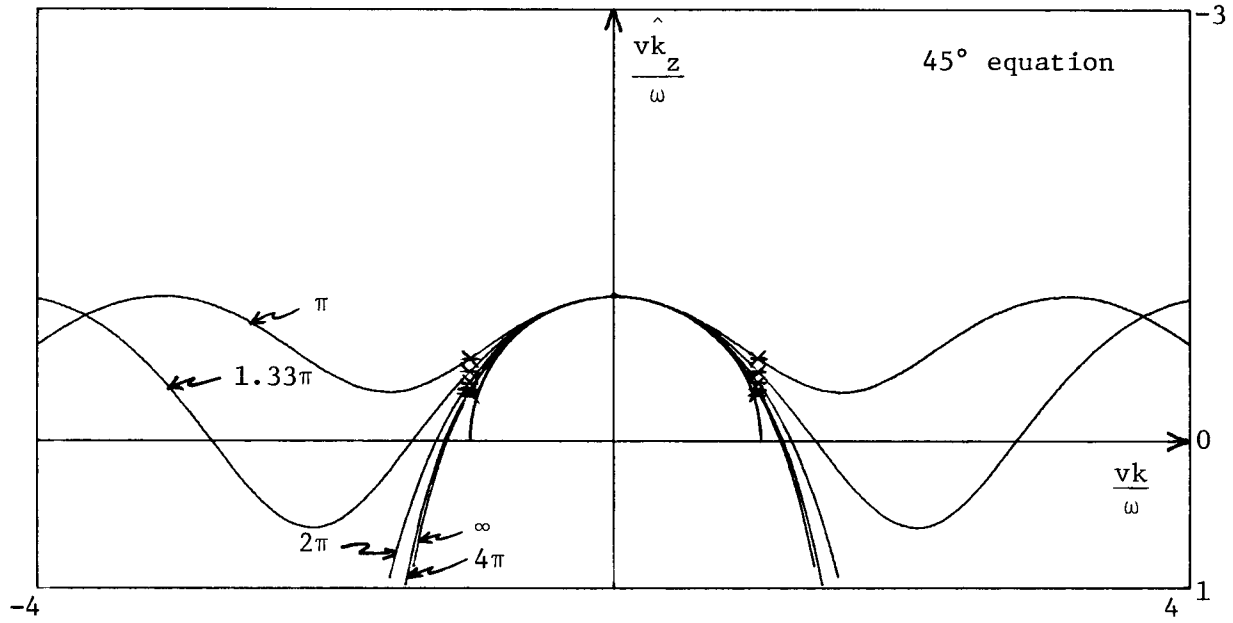

b

Figure 3. Dispersion relation $\frac{v\hat{k}_z}{\omega}$ vs. $\frac{vk}{\omega}$ for range of values of $m = \frac{2v}{\omega \Delta x}\pi$ for a) the 15° equation and b) the 45° equation. Effective horizontal wave number is $\hat{k} = \frac{2}{\Delta x} \sin\left(\frac{k \Delta x}{2}\right)$. Numbers beside arrows are values of m. $m = \infty$ implies no aliasing and no frequency dispersion. The asterisks represent $\frac{vk}{\omega} = \pm 1$ and ideally should lie on the $\frac{vk}{\omega}$ axis. The semi-circle is the dispersion relation for the exact wave equation. Compare with Figure 1a.

dependent upon m. The higher order 45° approximation (Fig. 3b) fits the exact dispersion relation ($m=\infty$) better for lower values of m than the 15° approximation. However, the rate of departure from the $m=\infty$ curve is more rapid after m becomes less than $\sim 1.3\pi$. In other words, although the $m=2\pi$ curves differ substantially for the 15° and 45° approximation, there is little difference in the $m=\pi$ curves. Thus, if $m \leq \sim \pi$, there is little gained in going from the 15° to the 45° approximation. Note that the typical case of $m=1$ is worse than any of the cases plotted.

The effect of using the bilinear transform to approximate k is shown in Figure 4. For the 15° approximation the effect of decreasing m is to pinch the dispersion curve towards the $\frac{v\hat{k}_z}{\omega}$ axis, which actually is the correct direction to better approximate the semi-circle dispersion relation of the exact wave equation. For $m \leq \sim 2\pi$, the dispersion relation lies inside the ideal semi-circle.

Group velocity

Consider a point source at $(x=0, z=0)$ in a homogeneous media of velocity v. If we take a picture of the wave front on time $t=1$ we will find a circle of radius v, or a semi-circle in the case of upgoing waves. Using our approximations to the wave equation we can also find the wave front by plotting $(x, -z) = tv(-\hat{s}_k/\hat{s}_\omega, -1/\hat{s}_\omega)$, where $\hat{s}_\omega = \frac{\partial \hat{k}_z}{\partial \omega}$ and $\hat{s}_k = \frac{\partial \hat{k}_z}{\partial k}$.

For $\delta_{xx} = (1, -2, 1)$ we need only equations (7c) and (7d). The wave fronts are plotted in Figure 5 for both 15° and 45° approximations and for several m's. Consider first the curves for $m=\infty$.

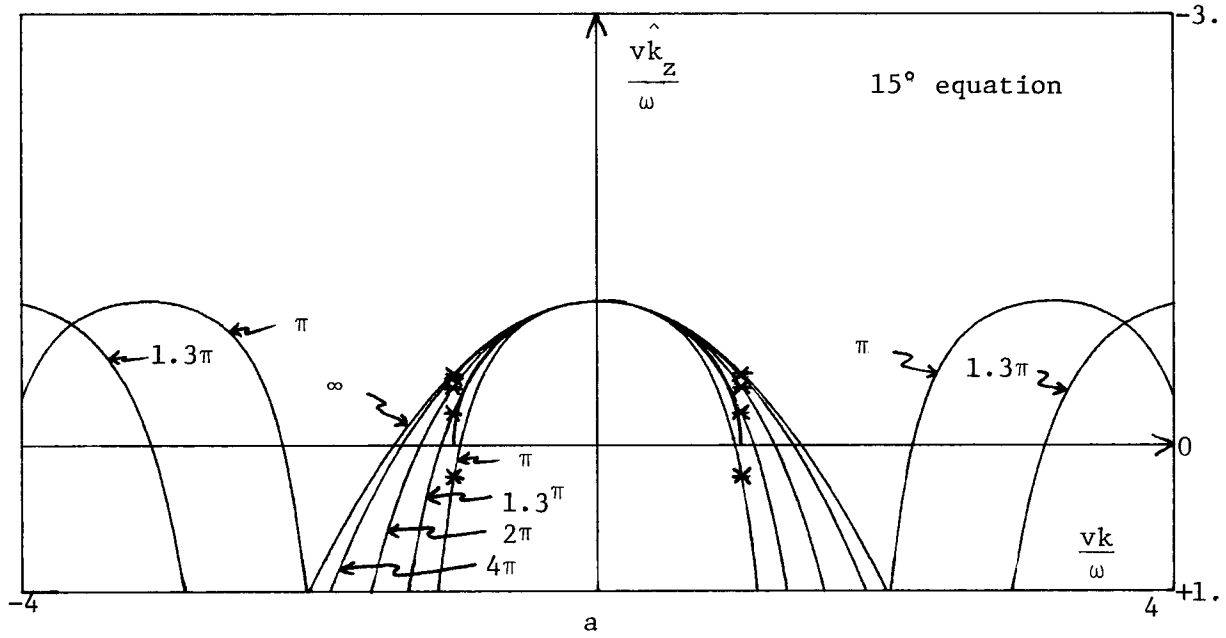

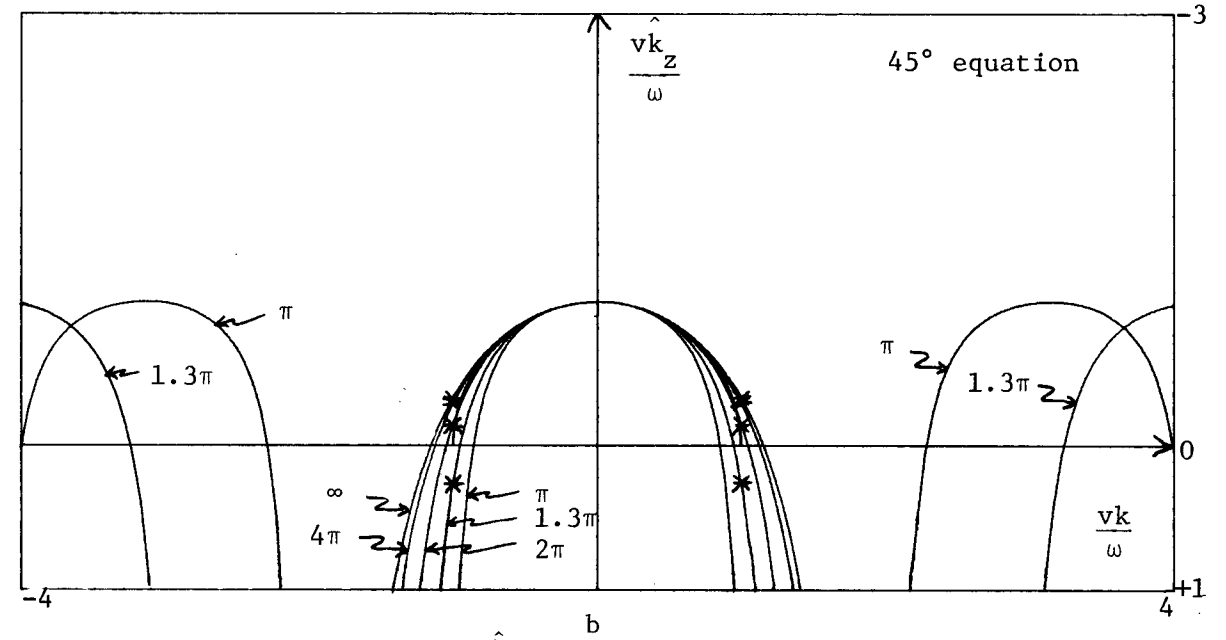

Fig. 4. Dispersion relation $\frac{\hat{vk}_z}{\omega}$ vs. $\frac{vk}{\omega}$ for range of values of $m = \frac{2v}{\omega\Delta x}\pi$ for a) the 15° equation and 6) the 45° equation. Effective horizontal wave number is $\hat{k} = \frac{2}{\Delta x}\tan\left(\frac{k\Delta x}{2}\right)$. Numbers beside arrows are values of m. $m = \infty$ implies no aliasing and no frequency dispersion. The asterisks represent $\frac{vk}{\omega} = \pm 1$ and ideally should lie on the $\frac{vk}{\omega}$ axis. The semi-circle is the dispersion relation for the exact wave equation. Compare with Figure 1b.

Note first of all that the wavefronts fit the ideal semi-circle out to $\theta = 15°$ and $45°$ in Figure 5a and 5b respectively. Secondly, note that all of the energy lies above the x axis as it must, since we can only propagate energy in one direction with our one-way equations. The asterisks indicate rays which ideally should be traveling in the $\pm x$ direction (i.e. $\frac{kv}{\omega} = 1$). Points which do not lie between the asterisks on a given curve represent waves with $k > \frac{\omega}{v}$. In the exact wave equation waves with $k > \frac{\omega}{v}$ are evanescent. We see, however, that these waves are propagated by the approximations to the wave equation and are usually attenuated by fan-filtering or by means of numerical viscosity.

The effect of decreasing m is to condense the wave fronts towards the z axis with the result of deteriorating the fit to the exact wave equation for smaller θ's . Referring ahead to the knots in Figures 9 and 10, we see, for example, that for $m=\pi$, the 15° and 45° equations maintain 1% degree of accuracy in x only out to $\theta=12°$ and $\theta=15°$ respectively.

If the bilinear transform is used to take the x derivatives then the group velocity curves are obtained by inserting equations (8c) and (8d) into equation (9c). The results for the 15° and 45° equations are plotted in Figure 6. A comparison with Figure 5 shows that the effect of decreasing m is opposite from above, i.e., as m is decreased, the energy is pushed away from the z axis. With reference to the knots in Figures 11 and 12 for $m=\pi$, the 15° and 45° equations maintain an accuracy in x of 1% only out to $\theta=13°$ and $\theta=11°$ respectively. The cause for this apparent ambiguity is due to the opposite direction of the anisotropic and frequency dispersion errors and will be discussed shortly.

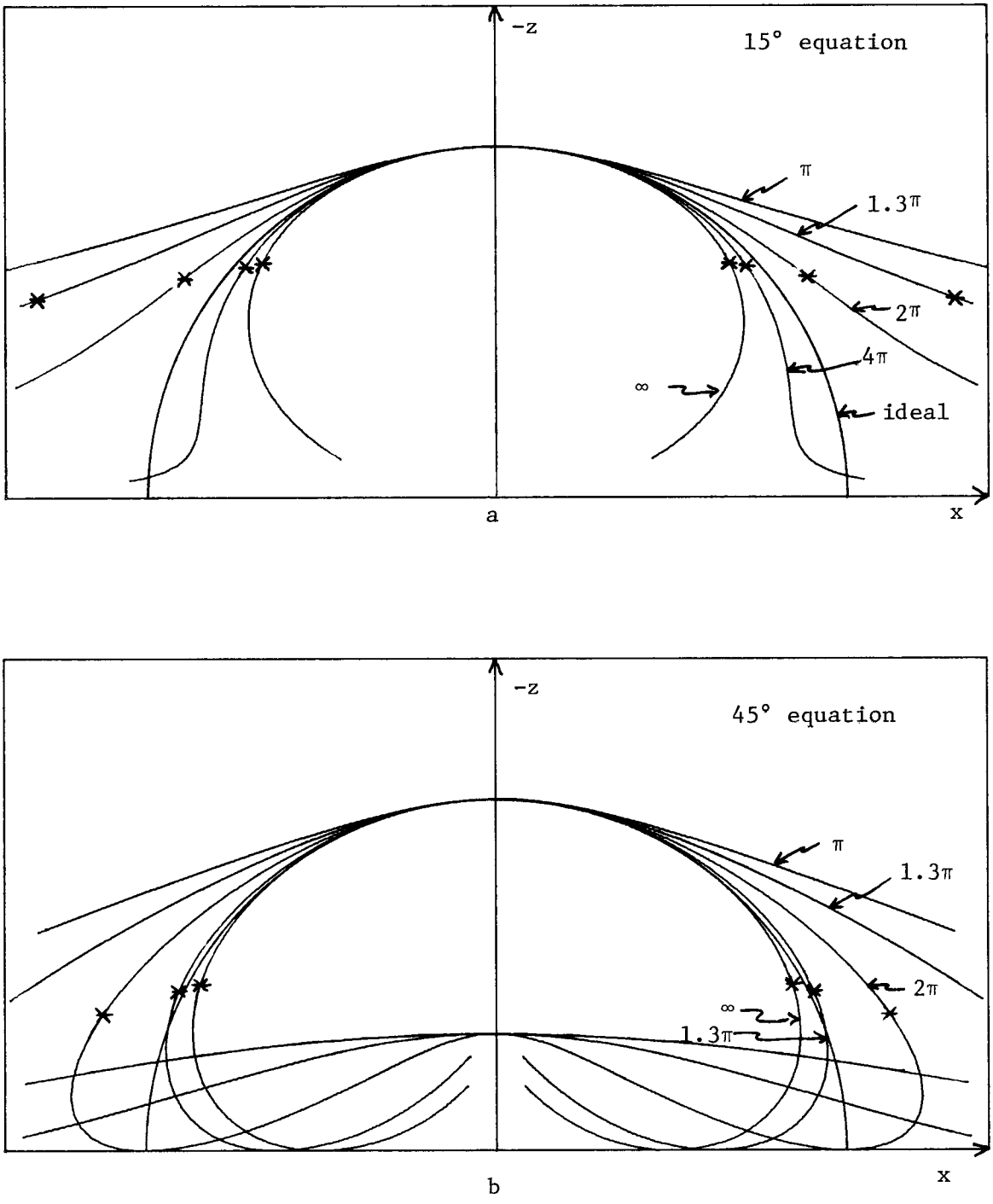

Fig. 6. Wavefronts in x,z space for a range of m's for a) the 15° equation and b) the 45° equation. Effective horizontal wave number is $\hat{k} = \frac{2}{\Delta x}\tan(\frac{k\Delta x}{2})$ Numbers beside arrows are values of m . Asterisks denote waves which ideally should be propagated horizontally in the $\pm$ x direction, i.e., $\frac{kv}{\omega} = \pm 1$. The semi-circle is the ideal wave front. Values of $\frac{kv}{\omega}$ between -1 and +1 lie between asterisks on upper portion of curves.

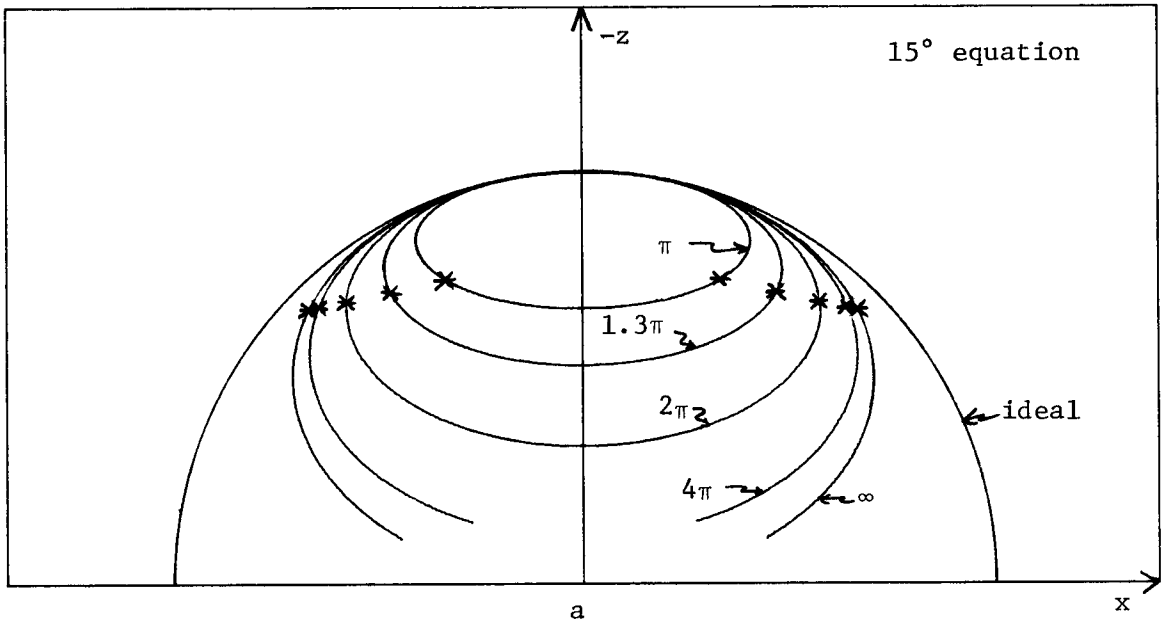

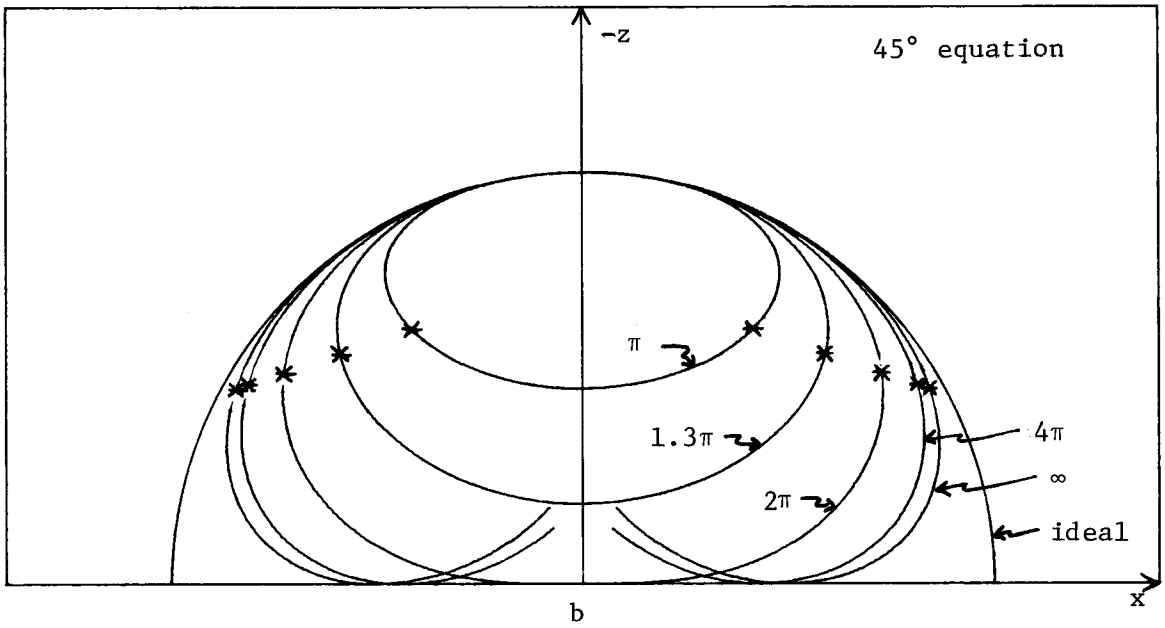

Fig. 5. Wavefronts in x,z space for a range of m's for a) the 15° equation and b) the 45° equation. Effective horizontal wave number is $\hat{k} = \frac{2}{\Delta x} \sin(\frac{k \Delta x}{2})$. Numbers beside arrows are values of m. Asterisks denote waves which ideally should be propagated horizontally in the $\pm$ x direction, i.e., $\frac{kv}{\omega} = \pm 1$. The semi-circle is the ideal wave front. Values of $\frac{kv}{\omega}$ between -1 and +1 lie between asterisks on upper portion of curves.

Travel time curves.

The travel time curves from a point scatterer for the 15° and 45° equations are shown in Figures 7 and 8 for $\hat{k} = \frac{2}{\Delta x} \sin(\frac{k \Delta x}{2})$ and $\hat{k} = \frac{2}{\Delta x} \tan(\frac{k \Delta x}{2})$ respectively. These curves are in the unprimed coordinate system. Going to the slant frames involves only a time shift since $\theta=0$. Because their character is so much like the group velocity curves we will leave these to the readers inspection. For reference, it should be mentioned that the asymptotes of the ideal travel time hyperbolas slope at angles of $\pm$ 45° .

Timing and distance errors.

We turn now to a final representation of the errors induced by sampling the x coordinate. Let Δx and Δt be the distance and timing errors caused by anisotropic and frequency dispersion. Claerbout, on page 12 , has shown that

$$(\Delta x, \Delta t) = z(-\frac{\partial}{\partial k}, \frac{\partial}{\partial \omega})(\hat{k}_z^j - k_z)$$

where we have added a hat to k_z^j to denote that this is the effective vertical wave number of the j^{th} approximation. k_z is the ideal vertical wave number from the exact wave equation. Δx and Δt are functions of the angle of propagation, θ , and can be thought of as the errors in migrating a true hyperbola.

Figure 9 shows Δx vs. Δt for the 15° equation for $\hat{k} = \frac{2}{\Delta x} \sin(\frac{k \Delta x}{2})$. The points plotted are at 4° intervals. The full scale range in errors is $\pm$ 1% for Δt and $\pm$ 3% for Δx . Note that positive Δt is down.

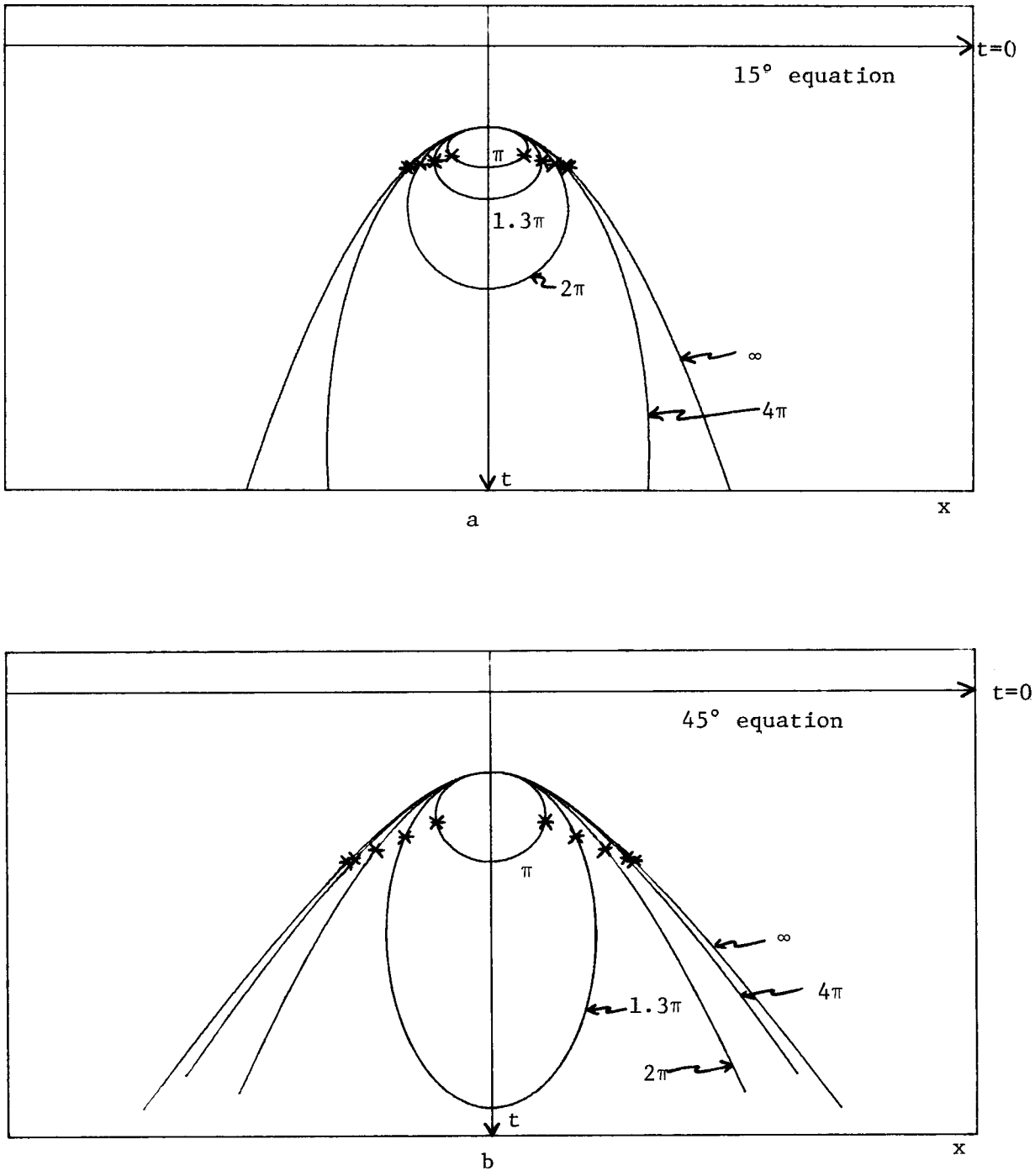

Fig. 7. Travel time curves due to point source for range of m's for a) 15° equation and 6) 45° equation. Effective wave number is $\hat{k} = \frac{2}{\Delta x}\sin(\frac{k\Delta x}{2})$. Numbers beside arrows are values of m's . Asterisks denote waves which ideally should be propagated horizontally in the $\pm$ x direction. Slope of asymptotes ideally should be $\pm$ 45°. Arrivals outside of asterisks are evanescent waves and should be attenuated by fan filtering or numerical viscosity. Compare with the wave fronts in Figure 5.

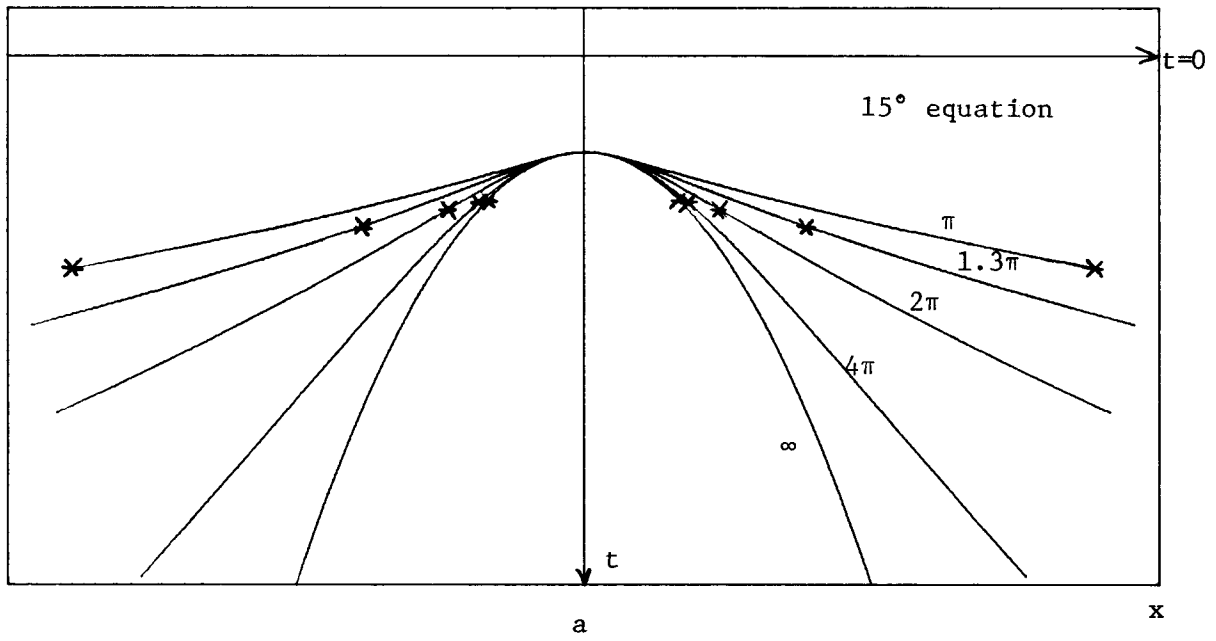

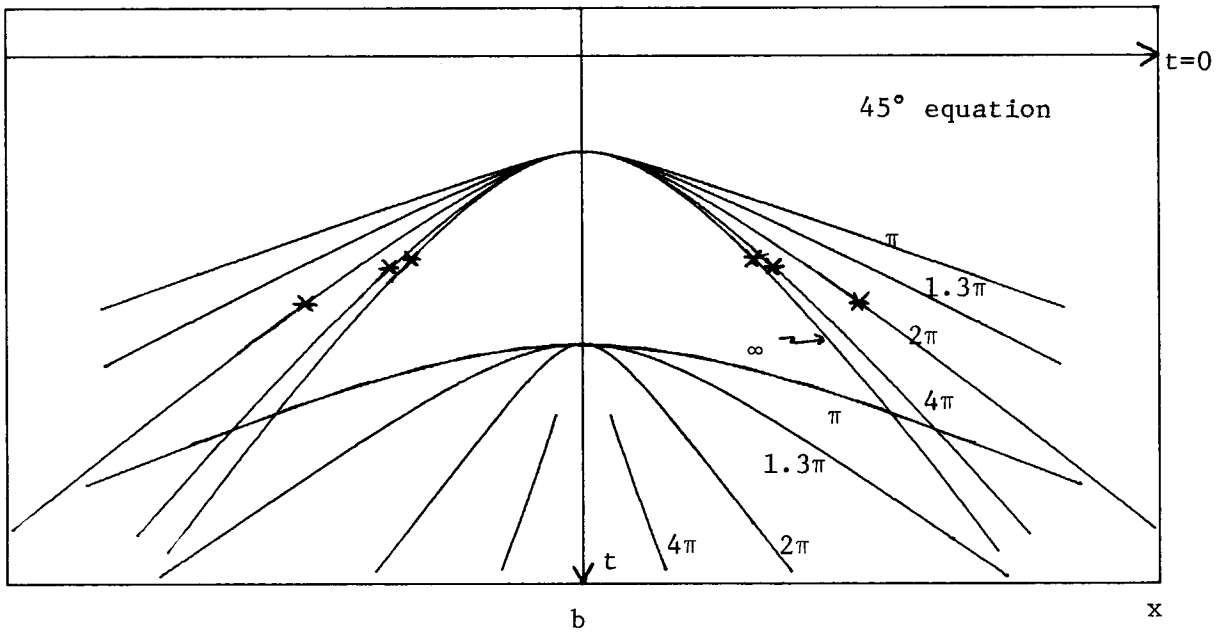

Fig. 8. Travel time curves due to point source for range of m's for a) 15° equation and b) 45° equation. Effective wave number is $\hat{k} = \frac{2}{\Delta x} \tan\left(\frac{k \Delta x}{2}\right)$. Numbers beside arrows are values of m's . Asterisks denote waves which ideally should be propagated horizontally in the $\pm$ x direction. Slope of asymptotes ideally should be $\pm$ 45° . Arrivals outside of asterisks are evanescent waves and should be attenuated by fan filtering or numerical viscosity. Compare with the wave fronts in Figure 6.

Figure 9a is for $m=\infty$ (i.e., continuous x) and thus represents the errors due to anisotropic dispersion alone. Figures 9b-d are for $m = 4\pi$, 2π, and π. The movement of the box for a given angle, θ, thus represents the error induced by sampling the x axis. The plots show that the direction of error is such that both Δx and Δt increase with decreasing m.

Figure 10 is the same plot using the 45° equation and shows a similar result. Note the higher degree of accuracy.

Figures 11-13 are for $\hat{k} = \frac{2}{\Delta x} \tan\left(\frac{k \Delta x}{2}\right)$ and are a little more interesting because of the opposite direction of the errors caused by anisotropic and frequency dispersion. Consider Figure 11 which is for the 15° equation. Figure 11a shows the error due to anisotropic dispersion alone (i.e. $m=\infty$). For the purpose of discussion let us follow the progress of the point corresponding to $\theta=12°$ as m is decreased. From the computer output from which the plots were generated we have the following table:

	15° equation	$\theta = 12°$
m	Δt	Δx
∞	0.00073	-0.00464
4π	0.00069	-0.00389
2π	0.00057	-0.00162
π	0.00009	+0.00779
$.8\pi$	-0.00021	+0.01521

A similar result holds for the other θ's. Hence, decreasing m moves Δx and Δt back towards zero total error and beyond. That is, the Δx, Δt error due to frequency dispersion works against the Δx, Δt error due to anisotropic dispersion and begins to dominate at some value of m, depending on θ.

Figure 12 shows the analogous plots for the 45° equation. However, because the anisotropic dispersion error is smaller due to the better approximation, the frequency dispersion error begins to dominate at larger values of m. Recall in the group velocity discussion that we mentioned that the Δx error is less than 1% for $\theta \leq 13°$ for the 15° approximation and $\theta \leq 11°$ for the 45° approximation. This ambiguity is thus explained by the above observation.

Knots can be computed for non-zero θ's also. Figure 13 shows the knots for the 15° equation with $\hat{k} = \frac{2}{\Delta x} \tan\left(\frac{k \Delta x}{2}\right)$. The dispersion relation is chosen to fit exactly at $\theta=20°$. The results are analogous to the previous plots and are left to the reader's inspection.

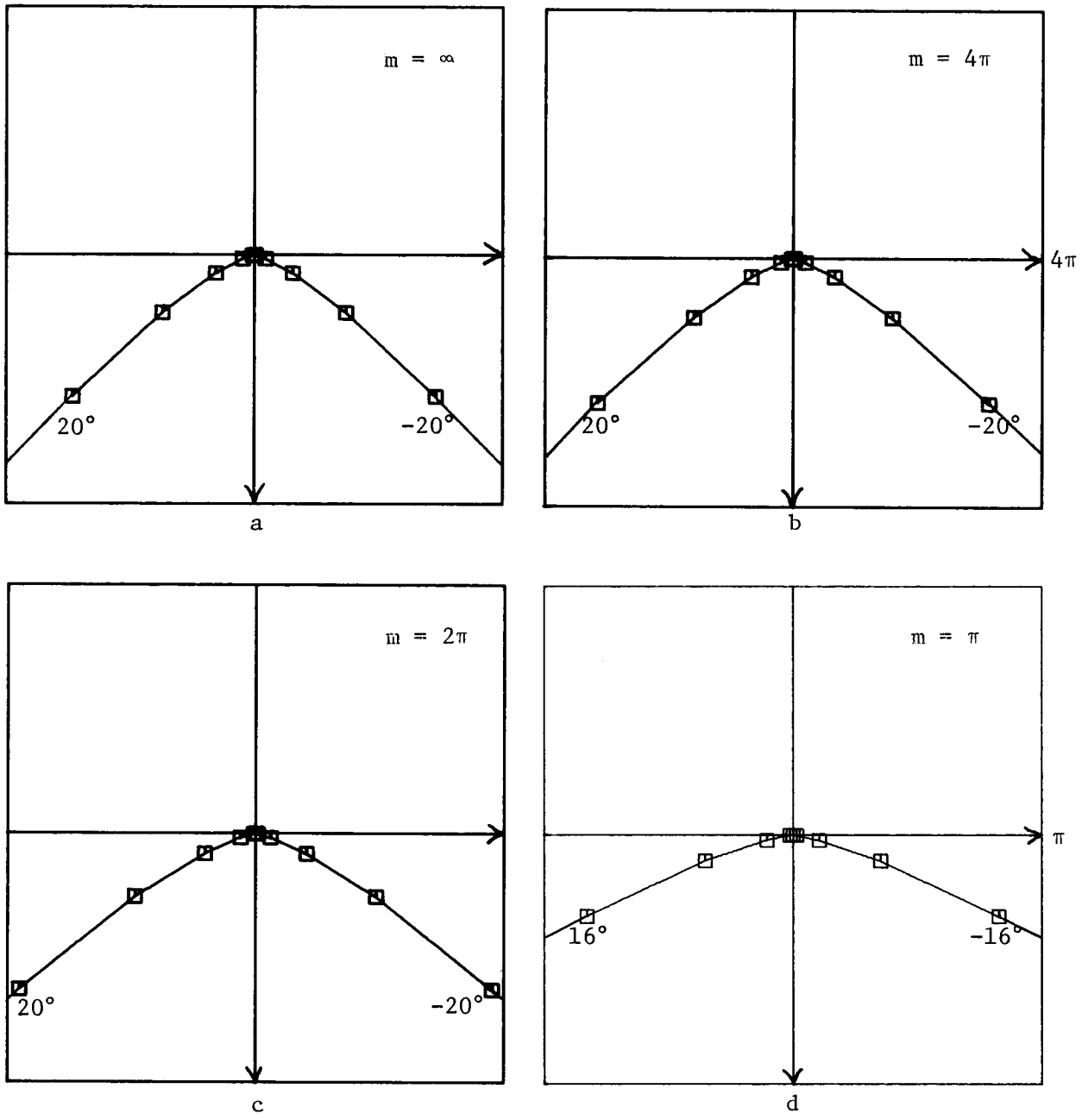

Fig. 9. Δx and Δt errors (knots) in migrating an ideal hyperbola using the 15° equation for various values of m. Effective horizontal wave number is $\hat{k} = \frac{2}{\Delta x} \sin\left(\frac{k \Delta x}{2}\right)$. Boxes are at 4° intervals and indicate the error in migrating the waves from that direction. The knot for $m = \infty$ gives the errors due to anisotropic dispersion alone. Vertical and horizontal axes are Δt and Δx respectively with Δt positive down. Full scale is $\pm$ 1% in Δt and $\pm$ 3% in Δx. Following a box for a given angle as m decreases shows the frequency dispersion. See text for example.

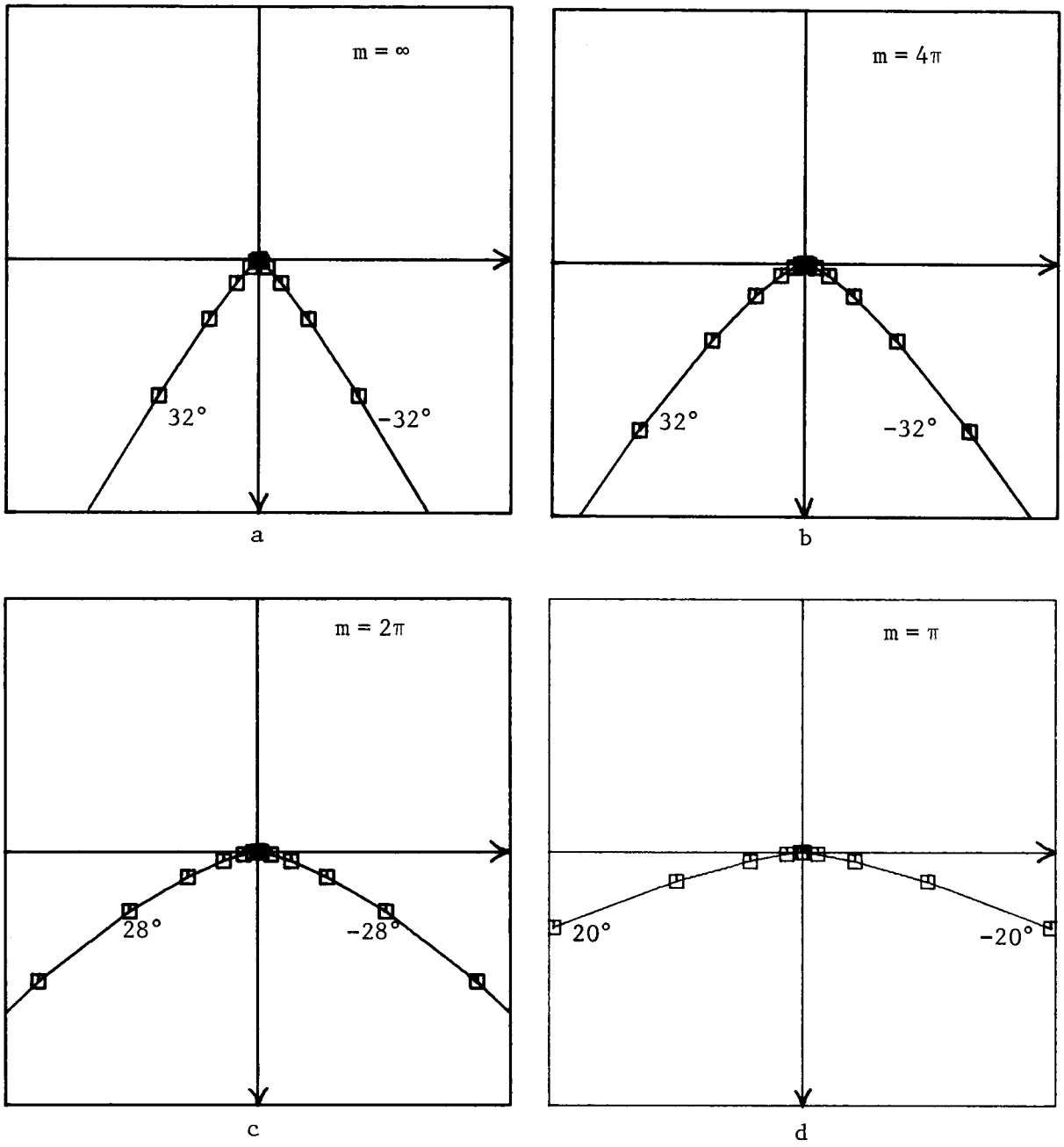

Fig. 10. Δx and Δt errors (knots) in migrating an ideal hyperbola using the 45° equation for various values of m. Effective horizontal wave number is $k = \frac{2}{\Delta x} \sin(\frac{k \Delta x}{2})$. Boxes are at 4° intervals and indicate the error in migrating the waves from that direction. The knot for $m = \infty$ gives the errors due to anisotropic dispersion along. Vertical and horizontal axes are Δt and Δx respectively with Δt positive down. Full scale is $\pm$ 1% in Δt and $\pm$ 3% in Δx. Following a box for a given angle as m decreases shows the frequency dispersion. See text for example.

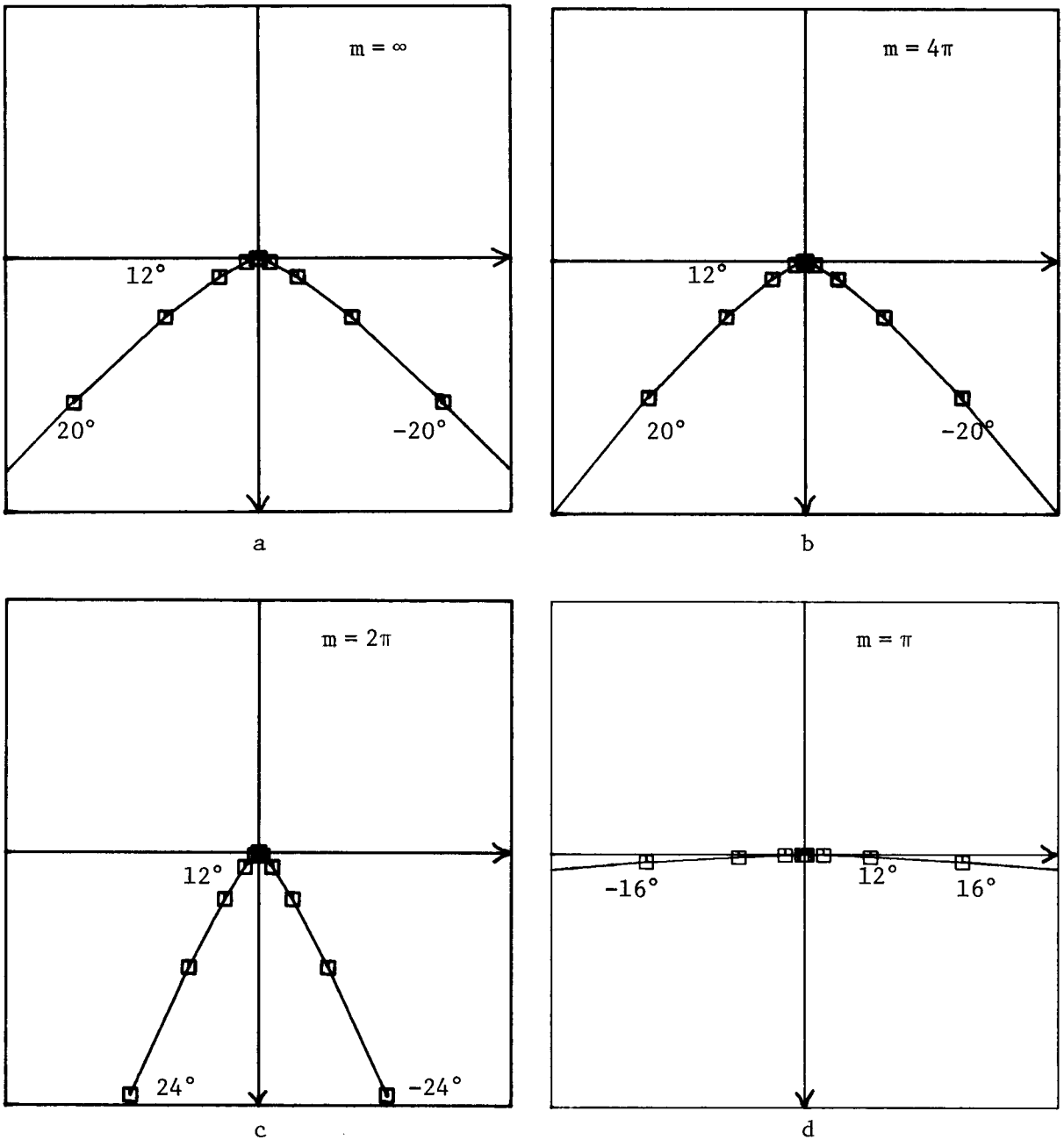

Fig. 11. Knots for 15° equation with effective horizontal wave number $k = \frac{2}{\Delta x} \tan\left(\frac{k\,\Delta x}{2}\right)$. Note that the limbs of the know have changed sign between $m = \pi$ and 2π. See Figure 9 caption for other details.

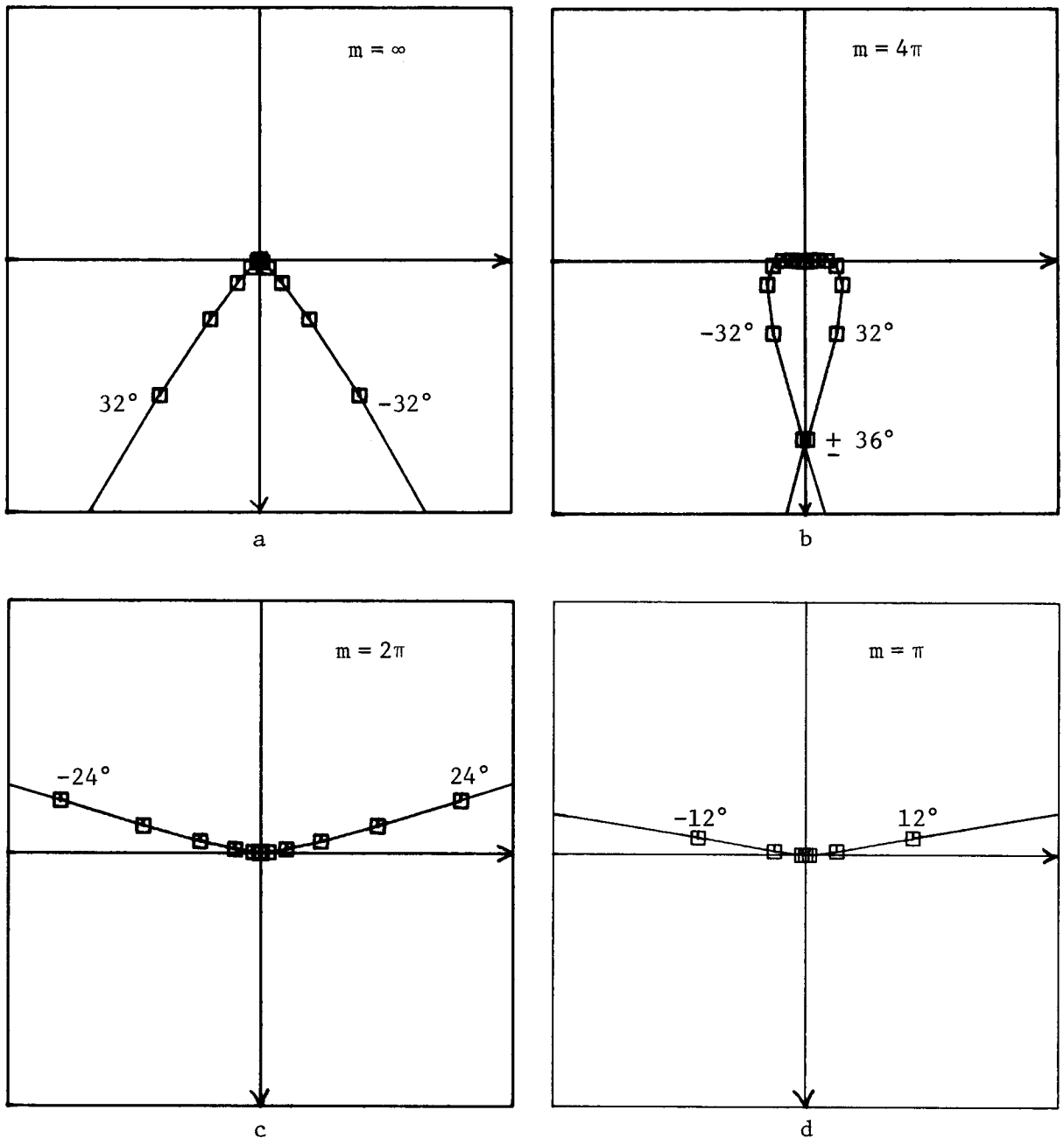

Fig. 12. Same as Fig. 11 but for 45° equation.

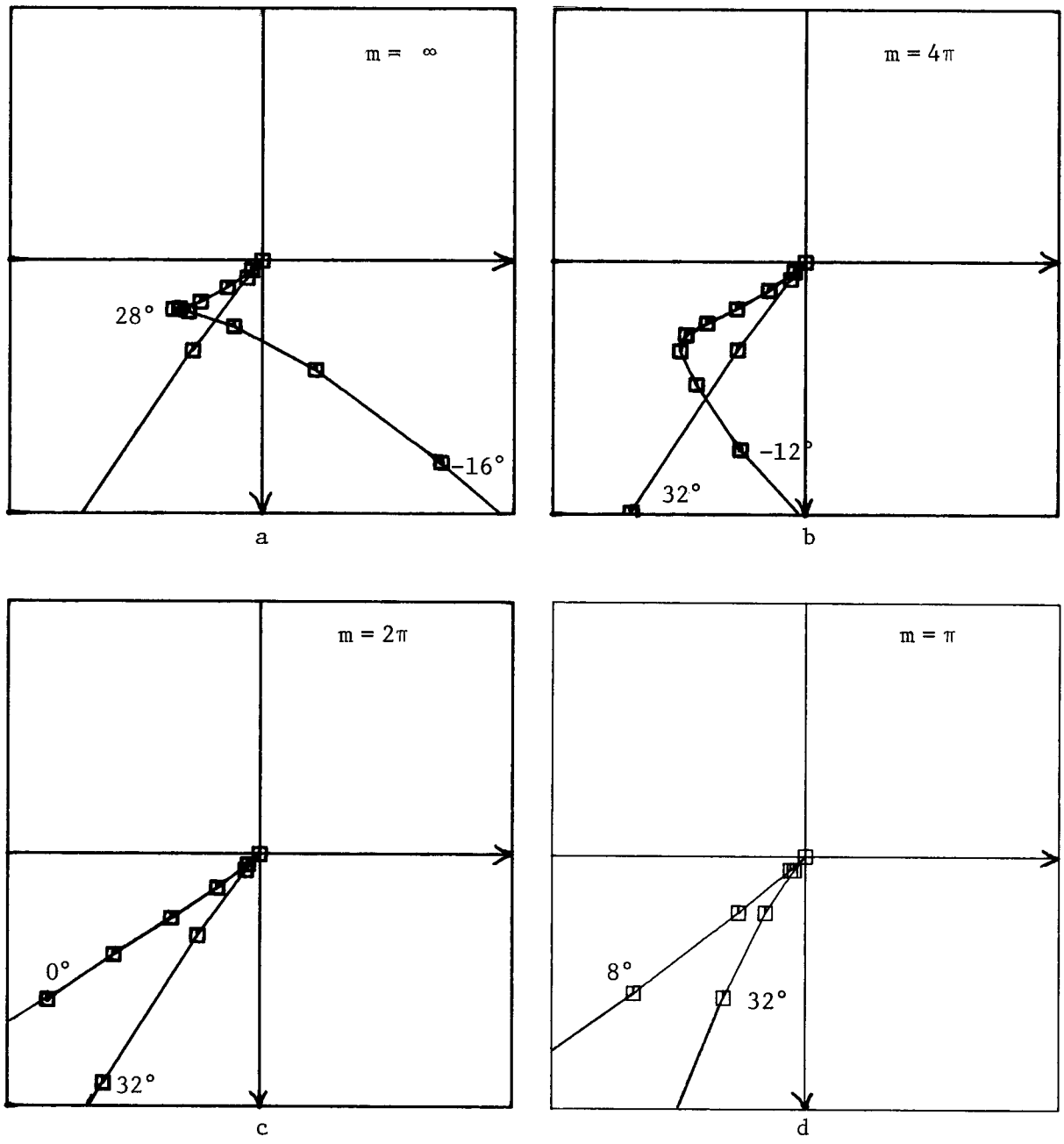

Fig. 13. Example of knot when dispersion relation is exactly fitted at a non-zero angle, in this case for $\theta = 20°$. See Figure 9 caption for details.